References and Notes

(1) (a) P. M. Maitlis, "The Organic Chemistry of Palladium", Vol. I and II, Academic Press, New York, 1971; (b) "Transition Metals in Homogeneous Catalysis", G. N. Schrauzer, Ed., Marcel Dekker, New York, 1971; (c) F. R. Hartley, "The Chemistry of Platinum and Palladium", Applied Science Publishers, London, 1973; (d) M. M. Taqui Khan and A. E. Martell, "Homogeneous Catalysis by Metal Complexes", Vol. II, Academic Press, New York, 1974.
(2) J. Tsuji, *Acc. Chem. Res.*, **2**, 144 (1969); **6**, 8 (1973).
(3) P. M. Henry, *Acc. Chem. Res.*, **6**, 16 (1973).
(4) (a) J. Tsuji, H. Takahashi, and M. Morikawa, *Tetrahedron Lett.*, 4387 (1965); (b) *Kogyo Kagaku Zasshi*, **69**, 920 (1966).
(5) K. E. Atkins, W. E. Walber, and R. Manyik, *Tetrahedron Lett.*, 3821 (1970).
(6) K. Takahashi, A. Miyake, and G. Hata, *Bull. Chem. Soc. Jpn.*, **45**, 230 (1972).
(7) K. Takahashi, G. Hata, and A. Miyake, *Bull. Chem. Soc. Jpn.*, **46**, 1012 (1973).
(8) H. Onoue, I. Moritani, and S.-I. Murahashi, *Tetrahedron Lett.*, 121 (1973).
(9) B. M. Trost and T. J. Fullerton, *J. Am. Chem. Soc.*, **95**, 292 (1973).
(10) B. M. Trost, T. J. Dietsche, and T. J. Fullerton, *J. Org. Chem.*, **39**, 737 (1974).
(11) B. M. Trost, W. P. Conway, P. E. Strege, and T. J. Dietshe, *J. Am. Chem. Soc.*, **96**, 7165 (1974).
(12) B. M. Trost and L. Weber, *J. Am. Chem. Soc.*, **97**, 1611 (1975).
(13) B. M. Trost and P. E. Strege, *Tetrahedron Lett.*, 2603 (1974).
(14) B. M. Trost and P. E. Strege, *J. Am. Chem. Soc.*, **97**, 2534 (1975).
(15) B. M. Trost and T. J. Dietshe, *J. Am. Chem. Soc.*, **95**, 8200 (1973).
(16) (a) B. M. Trost, L. Weber, P. E. Strege, T. J. Fullerton, and T. J. Dietsche, *J. Am. Chem. Soc.*, **100**, 3416 (1978); (b) *ibid.*, **100**, 3426 (1978).
(17) L. S. Hegedus, T. Hayashi, and W. H. Darlington, *J. Am. Chem. Soc.*, **100**, 7747 (1978).
(18) (a) S. Sakaki, H. Kato, and T. Kawamura, *Bull. Chem. Soc. Jpn.*, **48**, 195 (1975); (b). S. Sakaki, N. Hagiwara, N. Iwasaki, and A. Ohyoshi, *ibid.*, **50**, 14 (1977).
(19) S. Sakaki, N. Kudou, and A. Ohyoshi, *Inorg. Chem.*, **16**, 202 (1977).
(20) S. Sakaki, K. Hori, and A. Ohyoshi, *Inorg. Chem.*, **17**, 3183 (1978).
(21) M. S. Gordon, *J. Am. Chem. Soc.*, **91**, 3122 (1969).
(22) S. Ehrenson and S. Seltzer, *Theor. Chim. Acta*, **20**, 17 (1971).
(23) (a) This neglect results in the neglect of both interactions between the Pd 4dπ and the CO π orbital and between the Pd 4dπ and the CO π^* orbital. It is, however, conceivable that the former interaction contributes little to the coordination, because both the Pd 4dπ and CO π orbitals are doubley occupied. Thus, the above neglect mainly results in the neglect of the latter interaction. In fact, this neglect increases the electron density of the Pd atom and reduces the electron density of the CO ligand as is shown in Table I. (b) Strictly, it is correct that, although the basis set of the B systems include the P 3d orbitals, the overlap integrals between the Pd 4dπ and the P 3dπ are neglected. However, the P 3d orbitals are excluded from the basis set in the B system, because the basis set including the P 3d orbitals becomes too large and MO calculations with such a large basis set are time consuming. The exclusion of the P 3d orbitals gave the same results as those obtained when the π back-donation was excluded. Thus, the present method seems reasonable.
(24) H. Fujimoto, S. Kato, S. Yamabe, and K. Fukui, *J. Chem. Phys.*, **60**, 572 (1974).
(25) A. E. Smith, *Acta Crystallogr.*, **18**, 331 (1965).
(26) A. E. Smith, *Acta Crystallogr., Sect. A, Suppl.*, **25**, 161 (1969).
(27) D. R. Russell, P. A. Tucker, and S. Wilson, *J. Organomet. Chem.*, **104**, 387 (1976).
(28) B. Åkermark, J. E. Bäckvall, A. Löwenborg, and K. Zetterberg, *J. Organomet. Chem.*, **166**, C33 (1979).
(29) N. Numata and H. Kurosawa, *J. Organomet. Chem.*, **131**, 301 (1977).
(30) ΔE_b is defined as follows: ΔE_b = [binding energy between the $PdL_1L_2^{n+}$ fragment and π-$C_3H_5^-$] − [binding energy between $PdCl_2$ and π-$C_3H_5^-$], where the L_1 and L_2 = Cl^-, PH_3, or CO.
(31) R. J. Goodfellow and L. M. Venanzi, *J. Chem. Soc. A*, 784 (1966).
(32) Strictly speaking, the extent of the ϕ_n–ϕ_3 mixing is proportional to $\beta_{3n}/(\epsilon_3 - \epsilon_n)$, where $\beta_{3n} = \sum_r \sum_s C_{3r}C_{ns}\langle r|H|s\rangle$. While the C_{ns} is constant for various reaction systems, the C_{3r} slightly depends on the kinds of π-allylpalladium complexes, and it becomes large as ϕ_3 becomes stable. As ϕ_3 becomes stable, β_{3n} slightly increases and $\epsilon_3 - \epsilon_n$ becomes small. Thus, the mixing becomes large mainly due to the $(\epsilon_3 - \epsilon_n)^{-1}$ quantity and slightly due to β_{3n}.
(33) Strictly speaking, the extent of this mixing is also proportional to $\beta_{2n}\beta_{3n}(\epsilon_2 - \epsilon_n)^{-1}(\epsilon_3 - \epsilon_n)^{-1}$, where $\beta_{2n}\beta_{3n} \simeq C_{2p}{}^{C}C_{3p}{}^{C}\langle p_\pi{}^{C}|H|p_\pi{}^{O}\rangle^2$. The product, $C_{2p}{}^{C}C_{3p}{}^{C}$, is not so much different among the complexes examined, while this value slightly increases as ϕ_3 becomes stable. Thus, the extent of the mixing is approximately proportional to $(\epsilon_3 - \epsilon_n)^{-1}(\epsilon_2 - \epsilon_n)^{-1}$.
(34) Although these mixings are, strictly speaking, proportional to $\beta_{1n}\beta_{3n}(\epsilon_1 - \epsilon_n)^{-1}(\epsilon_3 - \epsilon_n)^{-1}$ and $\beta_{2n}\beta_{4n}(\epsilon_2 - \epsilon_n)^{-1}(\epsilon_4 - \epsilon_n)^{-1}$, respectively, the $\beta_{2n}\beta_{4n}$ and $\beta_{1n}\beta_{3n}$ quantities are not so much different among the complexes. Furthermore, $\beta_{2n}\beta_{4n}$ is almost the same as $\beta_{1n}\beta_{3n}$; for example, $\beta_{2n}\beta_{4n} \simeq 0.18C_{p_\pi}{}^{O2}\langle p_\pi{}^{C}|H|p_\pi{}^{O}\rangle^2$, and $\beta_{1n}\beta_{3n} \simeq 0.16C_{p_\pi}{}^{O2}\langle p_\pi{}^{C}|H|p_\pi{}^{O}\rangle^2$, for $PdCl(PH_3)(\pi$-$C_3H_5)$ (A). Thus, to examine the $(\epsilon_1 - \epsilon_n)^{-1}(\epsilon_3 - \epsilon_n)^{-1}$ and $(\epsilon_2 - \epsilon_n)^{-1}(\epsilon_4 - \epsilon_n)^{-1}$ quantities is enough to investigate the relative extent of the ϕ_1–ϕ_3 and ϕ_2–ϕ_4 mixings.
(35) G. Klopman, *J. Am. Chem. Soc.*, **90**, 223 (1968).
(36) (a) C. E. Moore, "Atomic Energy Levels", *Natl. Bur. Stand. (U.S.), Circ.*, **No. 467** (1958); (b) J. Hinze and H. H. Jaffé, *J. Am. Chem. Soc.*, **84**, 540 (1962); (c) L. Di Sipio, E. Tondello, G. De Michelis, and L. Oleari, *Chem. Phys. Lett.*, **11**, 287 (1971); (d) G. Burns, *J. Chem. Phys.*, **41**, 1521 (1964). (e) The scaling factor = $0.5[(\gamma_{3s,3s,semi\text{-}emp}/\gamma_{3s,3s,theor}) + (\gamma_{3p,3p,semi\text{-}emp}/\gamma_{3p,3p,theor})]$, where $\gamma_{rr,theor}$ is the theoretically calculated value with STO. (e) E. Clementi and D. L. Raimondi, *J. Chem. Phys.*, **38**, 2686 (1963); (f) H. Basch and H. B. Gray, *Theor. Chim. Acta*, **4**, 367 (1966).

Nitrosomethane and Its Nitrone and Oxime Isomers. A Theoretical Study of 1,2- and 1,3-Intramolecular Hydrogen Shifts

Paul D. Adeney, Willem J. Bouma, Leo Radom,* and William R. Rodwell

Contribution from the Research School of Chemistry, Australian National University, Canberra, A.C.T. 2600, Australia.

Received May 2, 1979

Abstract: Ab initio molecular orbital theory with minimal (STO-3G), split-valence (4-31G), and split-valence plus polarization (6-31G$^+$, 6-31G^{++}) basis sets and with electron correlation incorporated using Møller-Plesset perturbation theory terminated at second (MP2) and third (MP3) order has been used to investigate the potential-energy surface connecting nitrosomethane (**1**) and formaldoxime (**2**, **3**). The reaction path (A) for the 1,3-sigmatropic hydrogen shift leading to *syn*-formaldoxime (**2**) has been examined and the corresponding transition-state structure (**5**) has been determined. The transition state (**6**) for the subsequent isomerization of *syn*-formaldoxime (**2**) to its more stable anti isomer (**3**) has also been determined. A second reaction path (B), involving the isomerization of nitrosomethane (**1**) to *anti*-formaldoxime (**3**) by means of two successive 1,2-hydrogen shifts, is found to proceed via formaldonitrone (**4**) as an intermediate. The transition states (**7** and **8**) for the individual 1,2-hydrogen shifts have been determined. Both reaction paths A and B are found to involve high activation barriers, the rearrangement via the nitrone **4** being slightly favored. These results demonstrate the stability of nitrosomethane with respect to intramolecular rearrangement and also suggest that formaldonitrone might be amenable to experimental observation. STO-3G and 4-31G optimized structures for **1**-**8** are reported.

Introduction

Nitrosomethane is known to be less stable than its isomer formaldoxime and original attempts to isolate this molecule failed owing to its speedy isomerization to formaldoxime. More recently, however, the dimer of nitrosomethane has been prepared,[2-4] and has been shown in the gas phase to be in equilibrium with the monomer.[5] In 1968, the microwave

0002-7863/80/1502-4069$01.00/0

Table I. Calculated Total Energies (hartrees)[a] for Optimized Nitroso, Oxime, and Nitrone Isomers (**1–4**) and the Related Transition States (**5–8**)[b,c]

level	nitrosomethane (**1**)	*syn*-formaldoxime (**2**)	*anti*-formaldoxime (**3**)	formaldonitrone (**4**)
RHF/STO-3G[d]	−166.653 73	−166.643 49	−166.652 25	−166.566 79
RHF/4-31G[d]	−168.560 66	−168.570 04	−168.584 17	−168.552 06
RHF/4-31G	−168.564 79	−168.574 48	−168.588 55	−168.558 12
RHF/6-31G	−168.740 05	−168.748 46	−168.762 47	−168.733 58
RHF/6-31G$^+$	−168.825 90	−168.824 16	−168.833 78	−168.800 25
RHF/6-31G^{++}	−168.830 37	−168.835 77	−168.845 13	−168.807 53
MP2/6-31G^{++}	−169.319 47		−169.332 62	−169.303 71
MP3/6-31G^{++}	−169.333 73		−169.349 26	−169.314 09
level	TS: 1,3 H-shift **5**	TS: syn → anti **6**	TS: 1,2 H-shift **7**	TS: 1,2 H-shift **8**
RHF/STO-3G[d]	−166.498 81	−166.636 72	−166.465 92	−166.477 06
RHF/4-31G[d]	−168.415 64	−168.567 92	−168.438 46	−168.474 07
RHF/4-31G	−168.424 47	−168.572 21	−168.443 51	−168.473 88
RHF/6-31G	−168.599 37	−168.746 00	−168.619 63	−168.646 92
RHF/6-31G$^+$	−168.683 99	−168.819 60	−168.705 80	−168.704 09
RHF/6-31G^{++}	−168.694 61	−168.831 60	−168.715 48	−168.719 55
MP2/6-31G^{++}	−169.217 93		−169.223 60	−169.230 99
MP3/6-31G^{++}	−169.220 94		−169.229 64	−169.237 02

[a] 1 hartree = 2625.5 kJ mol^{-1}. [b] 4-31G optimized structures unless otherwise noted. [c] Structures labeled TS are transition states for the various rearrangements. [d] STO-3G optimized structures.

Scheme I

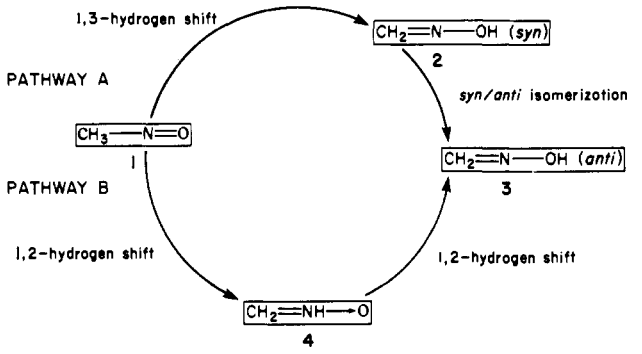

spectrum and the structure of nitrosomethane were reported,[6a] establishing nitrosomethane as a stable isomer of formaldoxime.

One mechanism for an intramolecular rearrangement of nitrosomethane to formaldoxime would be a 1,3-sigmatropic hydrogen rearrangement. In previous theoretical studies of such rearrangements, we have shown[7,8] that they require high activation energy, a finding which is in agreement with orbital-symmetry considerations.[9] The nitrosomethane/formaldoxime rearrangement, however, is particularly interesting, since there is also the possibility of nitrosomethane rearranging to formaldoxime by successive 1,2-hydrogen shifts, via formaldonitrone as an intermediate. Thus we have two possible pathways (A and B, Scheme I) for the rearrangement. Note that we have included in pathway A the isomerization of *syn*-formaldoxime to its anti isomer since microwave spectral studies[10,11] have shown that the anti form is the more stable isomer.

The aim of the present study is to examine the structures and energies of nitrosomethane (**1**), *syn*- and *anti*-formaldoxime (**2** and **3**, respectively), and the intermediate, formaldonitrone (**4**), as well as the four transition states (**5–8**) involved in pathways A and B, i.e., to investigate the intramolecular reaction potential surface connecting nitrosomethane with *anti*-formaldoxime. There have been several previous ab initio molecular orbital calculations on nitrosomethane,[12-19] formaldoxime[12,14,15,20-23] and formaldonitrone.[12] Most of these calculations were carried out with experimental, assumed, or standard geometries, and were concerned largely with the individual stable isomers and associated conformational problems. None of the previous studies examined the hydrogen-shift rearrangements described here.

Method and Results

Standard ab initio LCAO-SCF calculations were performed initially with a modified version[24] of the GAUSSIAN 70 system of programs[25] and the STO-3G[26] and 4-31G[27] basis sets. Full STO-3G and 4-31G geometry optimizations of structures **1–4** were carried out using a gradient optimization procedure,[28] subject only to a C_s symmetry constraint. The geometries of the transition states for the 1,3-hydrogen shift connecting nitrosomethane and formaldoxime (**5**), the syn/anti isomerization in formaldoxime (**6**), the 1,2-hydrogen shift connecting nitrosomethane and formaldonitrone (**7**), and the 1,2-hydrogen shift connecting formaldonitrone and formaldoxime (**8**), were obtained at the STO-3G and 4-31G levels by minimization of the gradient norm[29] while ensuring that the matrix of second derivatives of the energy had one negative eigenvalue. The optimized structures are displayed within the text, and include STO-3G values, 4-31G values (in parentheses), and, where available, experimental values (in square brackets) of the structural parameters.[30]

In order to obtain improved energy comparisons and to study the effect of basis-set enhancement and of electron correlation on the predicted relative energies, additional calculations were carried out on the 4-31G optimized structures. The 6-31G$^+$ and 6-31G^{++} basis sets (which are closely related to 6-31G* and 6-31G** basis sets[31]) were used. These involve respectively the addition to the standard 6-31G basis[32] of d-polarization functions on C, N, and O and the further addition of p-polarization functions on H, with polarization function exponents (ζ_{dC} = 0.626, ζ_{dN} = 0.923, ζ_{dO} = 1.292, ζ_{pH} = 0.75) taken from published optimization studies for correlated wave functions.[33] Valence-electron correlation was incorporated at the level of second-order (MP2) and third-order (MP3) Møller-Plesset perturbation theory.[33,34] The calculations were performed with the ATMOL3 system of programs[35] and an extended version[36] of Dykstra's SCEP program.[37] Calculated total energies obtained at both restricted Hartree-Fock (RHF) and correlation (MP2, MP3) levels are listed in Table I and relative energies are listed in Table II. Notation such as MP3/6-31G^{++} indicates an MP3 calculation with the 6-

Table II. Calculated Relative Energies (kJ mol^{-1}) for Optimized Nitroso, Oxime, and Nitrone Isomers (**1-4**) and the Related Transition States (**5-8**)[a,b]

level	nitroso-methane (**1**)	*syn*-formal-doxime (**2**)	*anti*-formal-doxime (**3**)	formaldo-nitrone (**4**)
RHF/STO-3G[c]	0	26.9	3.9	228.3
RHF/4-31G[c]	0	−24.6	−61.7	22.6
RHF/4-31G	0	−25.4	−62.4	17.5
RHF/6-31G	0	−22.1	−58.9	17.0
RHF/6-31G$^+$	0	4.5	−20.7	67.3
RHF/6-31G^{++}	0	−14.2	−38.7	60.0
MP2/6-31G^{++}	0		−34.5	41.4
MP3/6-31G^{++}	0		−40.8	51.6
level	TS: 1,3 H-shift **5**	TS: syn → anti **6**	TS: 1,2 H-shift **7**	TS: 1,2 H-shift **8**
RHF/STO-3G[b]	406.7	44.7	493.1	463.8
RHF/4-31G[b]	380.8	−19.1	320.8	227.3
RHF/4-31G	368.4	−19.5	318.4	238.7
RHF/6-31G	369.3	−15.6	316.1	244.5
RHF/6-31G$^+$	372.6	16.5	315.3	319.8
RHF/6-31G^{++}	356.4	−3.2	301.6	291.0
MP2/6-31G^{++}	266.6		251.7	232.3
MP3/6-31G^{++}	296.1		273.3	253.9

[a] All energies relative to nitrosomethane (**1**). [b] 4-31G optimized structures unless otherwise noted. [c] STO-3G optimized structures.

31G^{++} basis set. If the first field is omitted, an RHF calculation is implied. Geometries are indicated in some instances in the text by a double-bar separator: 4-31G//STO-3G means a 4-31G calculation on an STO-3G optimized structure.

Our best calculations are those at the MP3/6-31G^{++} level and we have used these to construct a reaction profile for both rearrangement pathways (A and B) as shown in Figure 1, except that the part of the profile referring to the syn → anti isomerization of formaldoxime is based on RHF/6-31G^{++} values. Unless otherwise stated, energy comparisons within the text refer to MP3/6-31G^{++} values.

Discussion

Optimized Structures and Relative Energies for the Nitroso, Oxime, and Nitrone Isomers. Nitrosomethane (**1**) is known from experimental[6] and previous theoretical[13,16,18,19] studies to have a preferred conformation in which the N=O bond is eclipsed by a neighboring C—H bond of the methyl group. An optimized geometry (double ζ basis set) for **1** has been previously reported.[19] We report here the STO-3G and 4-31G geometries and energies. Examination of the structural parameters displayed in **1** shows that agreement with the experimental structure[6b] is good.

For formaldoxime we have optimized both the syn (**2**) and the anti (**3**) isomers. The syn/anti energy difference had been previously calculated[14,15] using standard[38] geometries, and the STO-3G and 4-31G basis sets, yielding values of 24 and 45 kJ mol^{-1}, respectively, in favor of the anti isomer, whereas calculations[23] using floating spherical Gaussian orbitals (FSGO) produced a difference of 29 kJ mol^{-1}. STO-3G and 4-31G optimized structures of **3** have been reported;[22] however, no total energies were given. We have refined these parameters for **3** and have fully optimized **2**.

Total and relative energies shown in Table I demonstrate the fact that **3** is lower in energy than **2**, with the best estimate of the energy difference being 25 kJ mol^{-1} (6-31G^{++}). The optimized geometries for **3** can be compared with the experimentally determined structure.[11] The differences are small and characteristic of the basis sets employed (cf. ref 22). Formaldoxime is predicted to lie lower in energy than nitrosomethane. The calculated energy difference, however, is strongly influenced by the presence of polarization functions in the basis set (Table II). Addition of d functions to the 6-31G basis for C, N, and O (to yield 6-31G$^+$) preferentially favors the nitroso isomer (**1**) by a substantial 38.2 kJ mol^{-1}, while the further addition of p functions on H (yielding 6-31G^{++}) partly reverses this effect to the extent of 18.0 kJ mol^{-1}. We have observed very similar behavior in a study[39] of the related vinyl alcohol and acetaldehyde molecules and are in the process of generalizing our conclusions.[40] Electron correlation appears to have only a minor effect on the energy difference between **1** and **3**. Our best calculations (MP3/6-31G^{++}) predict that formaldoxime lies 41 kJ mol^{-1} below nitrosomethane.

Formaldonitrone (**4**) has not yet been observed experimentally, although its occurrence as an intermediate in the 1,3 cycloaddition of formaldoxime with monosubstituted alkenes[41] has been suggested. Isomer **4** is the parent compound of known substituted nitrones.[42-44] In agreement with the only previous ab initio study[12] on **4**, we find this isomer higher in energy (by

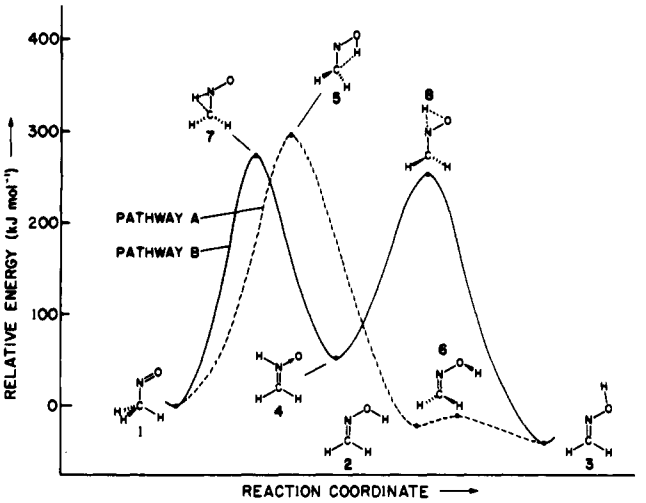

Figure 1. Reaction profile (constructed using MP3/6-31G^{++}//RHF/4-31G energies except that RHF/6-31G^{++}//RHF/4-31G values are used for the syn → anti isomerization) for the intramolecular rearrangement of nitrosomethane (**1**) to formaldoxime (**3**) by a 1,3-hydrogen shift (pathway A) or successive 1,2-hydrogen shifts (pathway B).

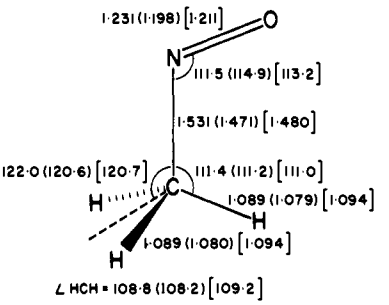

1

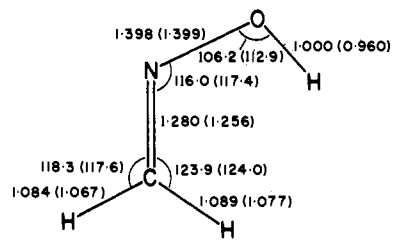

2

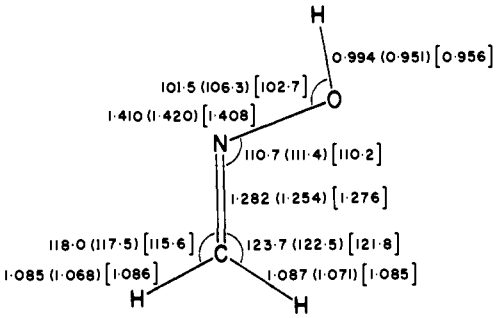

3

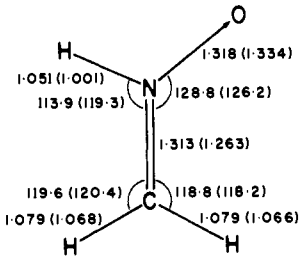

4

52 kJ mol^{-1}) than its nitroso isomer **1**. We note that the relative energies obtained at the STO-3G level do not describe the energy differences at all well (Table II). In addition, as with formaldoxime, the energy of formaldonitrone relative to nitrosomethane is strongly influenced by polarization functions. On the other hand, the energy of formaldonitrone relative to formaldoxime shows considerably smaller variation with change of basis set and incorporation of electron correlation, suggesting similar effects for these two systems (**3** and **4**) and a somewhat different effect in **1**. The optimized geometries of **4** are reasonably consistent with the results of an X-ray study[45] of *N*-methyl-*p*-chlorophenylnitrone: r(CN) = 1.309 Å, r(NO) = 1.280 Å, and ∠CNO = 125.5°.

Rearrangement of Nitrosomethane. Pathway A. In previous studies[7,8] of 1,3-sigmatropic hydrogen shifts, we have found substantial barriers for such rearrangements. Even though an antarafacial hydrogen shift is classified as "allowed" from orbital-symmetry considerations,[9] it seems that the steric problems involved in such a strained transition state contribute to a high energy of activation. The transition state (**5**) for the 1,3-hydrogen shift in the nitrosomethane (**1**)/formaldoxime (**2**) system is found to be quite high in energy, being 296 kJ mol^{-1} above **1**. The moving hydrogen (H_1) is clearly bonded simultaneously to the carbon and the oxygen in **5** as demonstrated by the small CNO angle (cf. the CNO angles in **1** and **2**).

The 1,3-hydrogen rearrangement leads to the formation of the syn isomer (**2**) of formaldoxime. This is not the most stable isomer of formaldoxime and we have, therefore, also investigated the transition state (**6**) for the subsequent isomerization to the preferred anti isomer (**3**) involving a rotation about the N–O bond. The transition state for rotation from *syn*-formaldoxime occurs for ∠H_1ONC = 54°, and the barrier is calculated to be only 11.0 kJ mol^{-1} (6-31G^{++}, Table II). A somewhat larger barrier (19.2 kJ mol^{-1}) was obtained in a recent FSGO study[23] but is considered less reliable than that of the present work because of the smaller basis set and use of a rigid rotor approximation in the FSGO calculations. Experimentally, there is little known about the syn/anti isomerization since the only observed species is *anti*-formaldoxime.[10,11,46] The overall reaction profile for this isomerization of **1** to **3** is shown as pathway A in Figure 1.

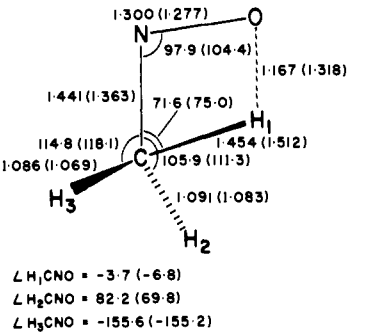

5

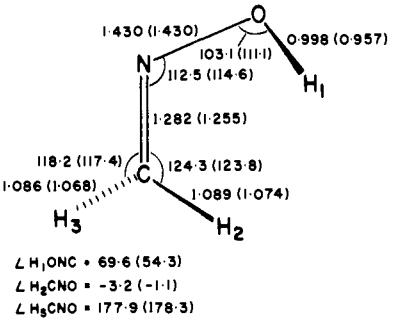

6

Rearrangement of Nitrosomethane. Pathway B. In our examination of this reaction pathway, we have first located the transition state (**7**) for the initial 1,2-hydrogen shift, corresponding to the isomerization of nitrosomethane (**1**) to its nitrone isomer (**4**). The position of the moving hydrogen (H_3) in the calculated transition state (**7**) is quite sensitive to the basis set employed. This can be explained by the fact that, at the STO-3G level, the nitrone (**4**) is much higher in energy than nitrosomethane (**1**) (see Table I). In agreement with the

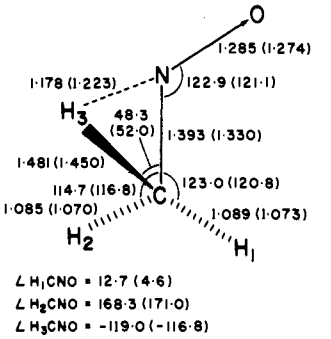

7

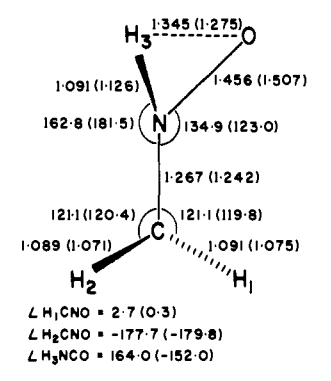

8

Hammond postulate,[47] we find a structure for **7** resembling more closely the higher energy isomer **4**. At the 4-31G level, the energy difference between **1** and **4** has decreased, which is reflected in the detailed structure of **7**. Note particularly the position of the bridging hydrogen (H_3). The calculated barrier is quite high (273 kJ mol^{-1}), but slightly less than the barrier for the 1,3-hydrogen shift.

The transition state (**8**) for the second 1,2-hydrogen shift is associated with the isomerization of formaldonitrone (**4**) to the more stable formaldoxime isomer (**3**). Again we find differences in the STO-3G and 4-31G structures of **8** which can be ascribed to the high relative energy of **4** at the STO-3G level. The position of the moving hydrogen (H_3) in **8** is in agreement with expectations based on the Hammond postulate. The calculated barrier for the isomerization of **4** to **3** is somewhat lower than the barriers associated with transition states **5** and **7**, but is still substantial (202 kJ mol^{-1}). The reaction profile for pathway B is also included in Figure 1.

Comparison of Theoretical Procedures. Since the theoretical study of reaction potential surfaces and, in particular, of the structures and energies of transition states is still in its infancy, it would seem appropriate to make some general remarks concerning results at the various levels of theory employed here. Our results for the experimentally known structures **1** and **3** confirm the ability of both STO-3G and 4-31G to describe well the equilibrium geometries of stable molecules.[48] For the transition-state structures **5**–**8**, experimental information is obviously unavailable but it is useful to compare here the STO-3G and 4-31G results. The differences between the geometries determined at these two levels of theory are somewhat larger for the transition states than for the stable isomers. Nevertheless, as we shall see below, the STO-3G structures are sufficiently close that they are very useful from an energy standpoint. Relative energies at the STO-3G level are in poor agreement with the 4-31G values. This is not unexpected: STO-3G is well known[14,49] to fare badly in nonisodesmic[49] energy comparisons. On the other hand, the close correspondence between the 4-31G//STO-3G and 4-31G//4-31G relative energies is particularly pleasing. The agreement is good, even for the transition states for which we noted some differences between the geometries calculated at the two levels. Clearly it would be premature to conclude that it is sufficient to determine transition-state structures at the STO-3G level as a basis for reliable energy predictions at a higher level, nor would we expect that this should always be the case. However, when it is possible to do energy comparisons with STO-3G optimized structures, the 4-31G//STO-3G (or higher level//STO-3G) approach represents a substantial saving in computational expense.

Our higher level calculations show, for the stable isomers, that the energies of **2**, **3**, and **4** relative to **1** are increased by the addition of d functions to the basis set for C, N, and O but decreased by the addition of p functions on H. As noted above, we have observed closely related effects elsewhere.[39,40] Electron correlation, calculated in the MP3 approximation, has a relatively small effect (2–9 kJ mol^{-1}) on the relative energies of **1**–**4**. Activation energies for intramolecular rearrangement, as measured by appropriate relative energies for transition states **5**, **6**, and **8**, are influenced to a somewhat greater extent (30–60 kJ mol^{-1}) by electron correlation (MP3/6-31G^{++}). It is interesting to note that in almost all the cases examined here MP2 calculations appear to substantially "overcorrect" for correlation effects (as indicated by the MP3 results). Finally, we note that no qualitative conclusions are modifed in moving from RHF/4-31G to higher levels of theory.

Conclusions

In this paper, we have discussed the isomerization of nitrosomethane to *anti*-formaldoxime by means of a detailed ab initio study of the potential-energy surface associated with two possible pathways for intramolecular rearrangement. We note the following points:

(i) Rearrangement via a 1,3-hydrogen shift (pathway A) or via successive 1,2-hydrogen shifts (pathway B) requires high activation energy. Thus nitrosomethane is predicted to be quite stable with respect to intramolecular rearrangement. This agrees with experimental results: nitrosomethane is an observable isomer of formaldoxime.

(ii) The rotational isomerization of *syn*- to *anti*-formaldoxime is associated with a small energy barrier of 11 kJ mol^{-1} and is exothermic by about 25 kJ mol^{-1}.

(iii) Formaldonitrone, which is an intermediate in the isomerization pathway B, lies 52 kJ mol^{-1} higher in energy than nitrosomethane. It is separated from both nitrosomethane and formaldoxime by substantial potential energy barriers (222 and 202 kJ mol^{-1}, respectively), and therefore offers a reasonable prospect of experimental observation under appropriate conditions.

(iv) Close agreement is found for relative energies calculated at the 4-31G//STO-3G and 4-31G//4-31G levels, even for transition states.

(v) Inclusion of polarization functions in the basis set is necessary to describe accurately the relative energies of the stable isomers.

(vi) Electron correlation leads to a lowering (by 30–60 kJ mol^{-1}) in the calculated activation energies for intramolecular rearrangement.

(vii) MP2 calculations appear to overestimate the effect of electron correlation on calculated relative energies.

References and Notes

(1) Bamberger, E.; Seligman, R. *Chem. Ber.* **1903**, *36*, 685.
(2) Coe, C. S.; Doumani, T. F. *J. Am. Chem. Soc.* **1948**, *70*, 1516.
(3) Gowenlock, B. G.; Trotman, J. *J. Chem. Soc.* **1955**, 4190.
(4) Gowenlock, B. G.; Trotman, J. *J. Chem. Soc.* **1956**, 1670.
(5) Batt, L.; Gowenlock, B. G.; Trotman, J. *J. Chem. Soc.* **1960**, 2222.
(6) (a) Coffey, D.; Britt, C. O.; Boggs, J. E. *J. Chem. Phys.* **1968**, *49*, 591. (b) Turner, P. H.; Cox, A. P. *J. Chem. Soc., Faraday Trans. 2* **1978**, *74*, 533.
(7) Bouma, W. J.; Poppinger, D.; Radom, L. *J. Am. Chem. Soc.* **1977**, *99*, 6443.
(8) Bouma, W. J.; Vincent, M. A.; Radom, L. *Int. J. Quantum Chem.* **1978**, *14*, 767.
(9) Woodward, R. B.; Hoffmann, R. *Angew. Chem., Int. Ed. Engl.* **1969**, *10*, 781.
(10) Levine, I. N. *J. Mol. Spectrosc.* **1962**, *8*, 276.
(11) Levine, I. N. *J. Chem. Phys.* **1963**, *38*, 2326.
(12) Robb, M. A.; Csizmadia, I. G. *J. Chem. Phys.* **1969**, *50*, 1819.
(13) Kollman, P. A.; Allen, L. C. *Chem. Phys. Lett.* **1970**, *5*, 75.
(14) Radom, L.; Hehre, W. J.; Pople, J. A. *J. Chem. Soc. A* **1971**, 2299.
(15) Radom, L.; Hehre, W. J.; Pople, J. A. *J. Am. Chem. Soc.* **1971**, *93*, 289.
(16) Mochel, A. R.; Griffin, L. L.; Kramling, R. W.; Boggs, J. E. *J. Chem. Phys.* **1973**, *58*, 4040.
(17) Talberg, H. J.; Ottersen, T. *J. Mol. Struct.* **1975**, *29*, 225.
(18) Hehre, W. J.; Pople, J. A.; Devaquet, A. J. P. *J. Am. Chem. Soc.* **1976**, *98*, 664.
(19) Flood, E.; Pulay, P.; Boggs, J. E. *J. Am. Chem. Soc.* **1977**, *99*, 5570.
(20) Liotard, D.; Dargelos, A.; Chaillet, M. *Theor. Chim. Acta* **1973**, *31*, 325.
(21) Dargelos, A.; Liotard, D.; Chaillet, M. *Theor. Chim. Acta* **1975**, *38*, 79.
(22) Pouchan, C.; Liotard, D.; Dargelos, A.; Chaillet, M. *J. Chim. Phys. Phys.-Chim. Biol.* **1976**, *73*, 1046.
(23) Hwang, W. F.; Kuska, H. A. *J. Mol. Struct.* **1978**, *48*, 239.
(24) Poppinger, D.; Vincent, M. A.; Hinde, A. L.; Radom, L., unpublished.
(25) Hehre, W. J.; Lathan, W. A.; Ditchfield, R.; Newton, M. D.; Pople, J. A. Program No. 236, QCPE, University of Indiana, Bloomington, Ind., 1973.
(26) Hehre, W. J.; Stewart, R. F.; Pople, J. A. *J. Chem. Phys.* **1969**, *51*, 2657.
(27) Ditchfield, R.; Hehre, W. J.; Pople, J. A. *J. Chem. Phys.* **1971**, *54*, 724.
(28) Poppinger, D. *Chem. Phys. Lett.* **1975**, *34*, 332.
(29) Poppinger, D. *Chem. Phys. Lett.* **1975**, *35*, 550.
(30) Throughout this paper, bond lengths are in ångstroms and bond angles in degrees.
(31) Hariharan, P. C.; Pople, J. A. *Theor. Chim. Acta* **1973**, *28*, 213.
(32) Hehre, W. J.; Ditchfield, R.; Pople, J. A. *J. Chem. Phys.* **1972**, *56*, 2257.
(33) Pople, J. A.; Binkley, J. S.; Seeger, R. *Int. J. Quantum Chem., Quantum Chem. Symp.* **1976**, *10*, 1.
(34) Møller, C.; Plesset, M. S. *Phys. Rev.* **1934**, *46*, 618.
(35) Saunders, V. R.; Guest, M. F. "ATMOL3 Users Guide"; Science Research Council; Daresbury, Warrington, England.
(36) Rodwell, W. R., unpublished.
(37) Dykstra, C. E.; Schaefer, H. F.; Meyer, W. *J. Chem. Phys.* **1976**, *65*, 2740.
(38) Pople, J. A.; Gordon, M. S. *J. Am. Chem. Soc.* **1967**, *89*, 4253.

(39) Bouma, W. J.; Radom, L.; Rodwell, W. R., *Theor. Chim. Acta*, in press.
(40) Rodwell, W. R.; Radom, L., unpublished.
(41) Ochiai, M.; Obayashi, M.; Morita, K. *Tetrahedron* **1967**, *23*, 2641.
(42) Dobashi, T. S.; Goodrow, M. H.; Grubbs, E. J. *J. Org. Chem.* **1973**, *38*, 4440.
(43) Bjørgo, J.; Boyd, D. R.; Neill, D. C. *J. Chem. Soc., Chem. Commun.* **1974**, 478.
(44) Houk, K. N.; Caramella, P.; Munchausen, L. L.; Chang, Y.-M.; Battaglia, A.; Sims, J.; Kaufman, D. C. *J. Electron Spectrosc. Relat. Phenom.* **1977**, *10*, 441.
(45) Folting, K.; Lipscomb, W. N. *Acta Crystallogr.* **1964**, *17*, 1263.
(46) Azman, A.; Hadzi, D.; Kidric, J.; Orel, B. *Spectrochim. Acta* **1971**, *27*, 2499.
(47) Hammond, G. S. *J. Am. Chem. Soc.* **1955**, *77*, 334.
(48) See, for example, Pople, J. A. In "Modern Theoretical Chemistry", Schaefer, H. F., Ed.; Plenum Press: New York, 1977; Vol. IV, Chapter 1.
(49) Hehre, W. J.; Ditchfield, R.; Radom, L.; Pople, J. A. *J. Am. Chem. Soc.* **1970**, *92*, 4796.

A Theoretical Approach to the Birch Reduction. Structures and Stabilities of Cyclohexadienyl Radicals[1]

Arthur J. Birch, Alan L. Hinde, and Leo Radom*

Contribution from the Research School of Chemistry, Australian National University, Canberra, A.C.T. 2600, Australia. *Received October 15, 1979*

Abstract: Ab initio molecular orbital calculations with the minimal STO-3G basis set and restricted (RHF) and unrestricted (UHF) Hartree–Fock procedures have been carried out for a series of substituted cyclohexadienyl radicals (SCHD·). The structure of the unsubstituted cyclohexadienyl radical has been fully optimized and substituents (CH_3, CN, COOH, NO_2, COO^-, F, OCH_3, OH, and NH_2) have been sited in the 1, 2, 3, or 6 positions. The calculations indicate that the thermodynamically preferred site of protonation of a substituted benzene radical anion (corresponding to the most stable SCHD· isomer) is para to the substituent, except for the strong π donors (OH, OCH_3, and NH_2) and CH_3, where ortho protonation is favored. The thermodynamic predictions are compared with predictions of kinetically controlled protonation based on calculated molecular electrostatic potentials.

Introduction

The Birch reduction of substituted benzenes by alkali metals and alcohols in liquid ammonia is a reaction of widespread synthetic utility[2] (1). As part of a continuing study[1] of the

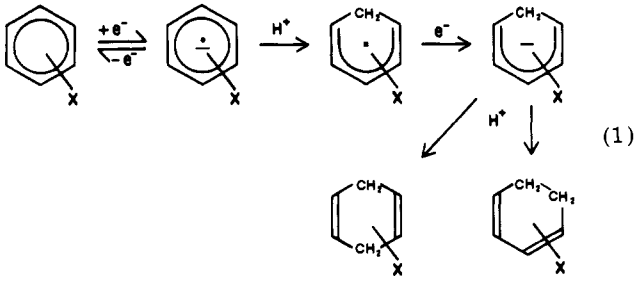

(1)

theory of the Birch reduction, we have previously examined in detail the reversible electron addition to substituted benzenes (SBz) yielding substituted benzene radical anions (SBz^-), and the subsequent irreversible protonation of the SBz^- systems. In this paper, we examine products of the first protonation step in the reaction sequence (1), namely, the substituted cyclohexadienyl radicals (SCHD·). Relative energies of isomeric SCHD·'s reflect the thermodynamically preferred protonation sites of the SBz^-'s. Although, under usual reaction conditions, this first protonation step is thought to be irreversible and hence subject to kinetic control,[3] a study of the thermodynamically preferred products allows a useful comparison with the kinetically preferred products as well as providing relative stabilities of the various SCHD· isomers.

The protonation reaction (2) has several possible isomeric outcomes depending on whether the proton adds ipso, ortho, meta, or para to the substituent X. We have previously argued[1b] that, under kinetic control, the preferred protonation sites are largely determined by electrostatic considerations, as reflected in minima of molecular electrostatic potential (MEP) maps.[1b,4] Relative rates, under such conditions, are

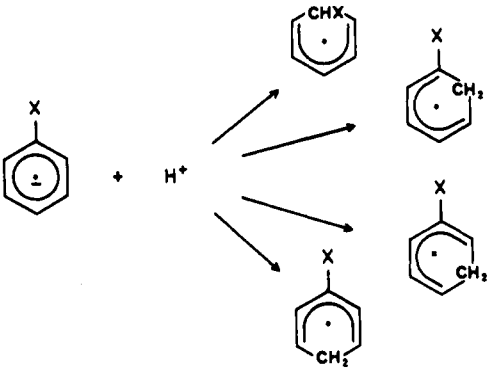

(2)

determined by the relative activation energies of protonation, and the activation energies in turn can be expected to be paralleled by the depths of the MEP minima. In contrast, under reversible conditions, the preferred protonation site is simply the thermodynamically most stable SCHD· isomer.

The main aims of this study are then to determine the thermodynamically preferred protonation sites of SBz^- and compare them with the MEP-controlled (kinetically controlled) sites on the one hand, and, on the other, to present and compare the energetics of the protonation reaction (2) with the depths of the MEP minima. The SCHD·'s are also of interest in their own right and comparisons of our findings are made with available experimental (ESR spectral and thermochemical) data.

Previous calculations[5-8] on CHD· have been aimed at producing spin densities and hyperfine coupling constants and vary in sophistication from simple valence bond to semiempirical procedures. The most sophisticated is an INDO semiempirical study[7] in which a complete geometry optimization of CHD· was carried out, and calculations on several fluoro-substituted derivatives were performed using the optimized structure. The motivation for these calculations was mainly a desire to interpret and confirm the ESR spectra of cyclohexadienyl rad-

0002-7863/80/1502-4074$01.00/0